

LEGO: Learning EGOcentric Action Frame Generation via Visual Instruction Tuning

Bolin Lai^{1,2†} Xiaoliang Dai¹ Lawrence Chen¹ Guan Pang¹ James M. Rehg³ Miao Liu¹
¹GenAI, Meta ²Georgia Institute of Technology ³University of Illinois Urbana-Champaign

bolin.lai@gatech.edu {xiaoliangdai, lawrencechen, gpang, miaoliu}@meta.com jrehg@illinois.edu

arXiv:2312.03849v1 [cs.CV] 6 Dec 2023

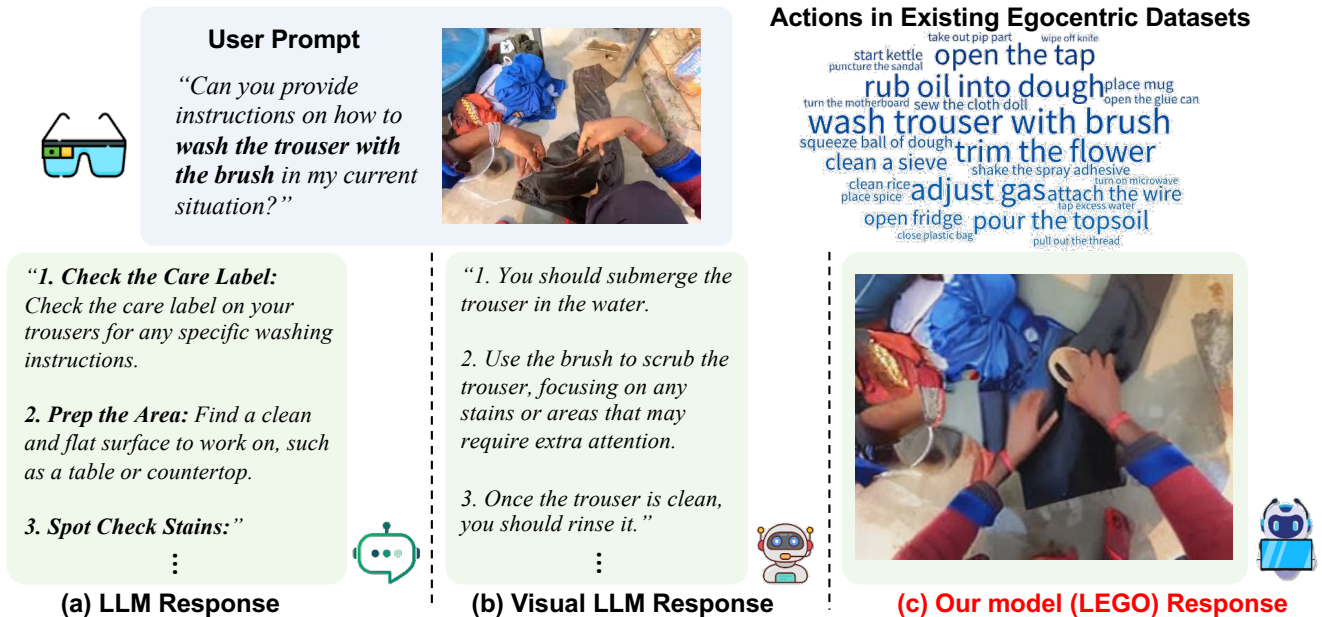


Figure 1. When the user queries for instructions on acquiring specific skills, large language models (LLMs) tend to provide general instructions that may not be readily applicable to the user’s current situation. While visual large language models (VLLMs) can generate more specific guidance based on visual prompt capturing the user’s context, the generated textual instructions still lack clarity and ease for the user to interpret. In contrast, we present a novel model — LEGO, which takes the user’s query and an egocentric image captured from user’s perspective as inputs. It then generates an egocentric action frame that vividly illustrates the execution of the query action.

Abstract

Generating instructional images of human daily actions from an egocentric viewpoint serves a key step towards efficient skill transfer. In this paper, we introduce a novel problem – egocentric action frame generation. The goal is to synthesize the action frame conditioning on the user prompt question and an input egocentric image that captures user’s environment. Notably, existing egocentric datasets lack the detailed annotations that describe the execution of actions. Additionally, the diffusion-based image manipulation models fail to control the state change of an action within the corresponding egocentric image pixel space. To this end, we finetune a visual large language model (VLLM) via visual instruction tuning for curating the enriched action de-

scriptions to address our proposed problem. Moreover, we propose to Learn EGOcentric (LEGO) action frame generation using image and text embeddings from VLLM as additional conditioning. We validate our proposed model on two egocentric datasets – Ego4D and Epic-Kitchens. Our experiments show prominent improvement over prior image manipulation models in both quantitative and qualitative evaluation. We also conduct detailed ablation studies and analysis to provide insights on our method.

1. Introduction

The emergence of Large Language Models (LLMs) [6, 10, 66, 99], such as ChatGPT, has revolutionized the transfer of knowledge. However, an LLM alone is not a sufficient

[†]This work was done during Bolin’s internship at GenAI, Meta.

tool for human skill transfer. Consider a question answering example in Fig. 1(a). The AI agent can summarize general world knowledge, yet it’s not directly applicable to the user’s current circumstance. On the other hand, the egocentric visual perception provides a novel means to capture the actions and intents as well as the surrounding contexts of the camera wearer. As shown in Fig. 1(b), recent Visual Large Language Models (VLLMs) [1, 12, 47, 53, 103] show the capability of generating instructional responses based on the egocentric visual prompt. However, the generated textual instructions are not the ideal vehicle for transferring human skills, as neuroscience studies have revealed that human brain processes images much faster than texts [4]. Moreover, it has also been evidenced that humans can interpret an action from a static image [23]. Motivated by these discoveries, we seek to design an egocentric AI system capable of synthesizing an image that not only vividly depicts how an action should be conducted, but also seamlessly aligns with the user’s visual perspective.

Formally, we introduce the novel problem of egocentric action frame generation as shown in Fig. 1(c). Given a user query of how to perform a specific action and an egocentric image capturing the moment before the action begins, the goal is to synthesize an egocentric image illustrating the execution of the action in the same egocentric context. In this paper, we address this problem by harnessing diffusion models [28, 69], which have shown strong capability in image manipulation tasks [5, 26, 45, 58, 101]. There are two major challenges in using diffusion models to generate action frames from an egocentric perspective. First, the action annotations of the existing egocentric datasets [13, 22] are simply composed of a verb and nouns (see Fig. 1), and thus lack the necessary details for diffusion models to learn the action state change and to associate the action with correct objects and body movements. Second, even when provided with detailed prompts about egocentric actions, conditioning solely from a text encoder may not be able to effectively control the action state change for action frame generation.

To address these challenges, we propose to Learn the EGOcentric (LEGO) action frame generation model with visual instruction tuning. First, we design a data curation pipeline that generates enriched action descriptions at scale, by finetuning a VLLM with visual instruction tuning. Second, we leverage the image and text embeddings from finetuned VLLM as a complement to the text encoder from the diffusion model to improve the controllability for action frame generation. Our experimental results suggest that the enriched action descriptions and the utilization of VLLM embeddings both improve the image generation performance. Overall, our contributions can be summarized as follows:

- We introduce the novel problem of egocentric action frame generation to facilitate the process of skill transfer.

- We leverage visual instruction tuning to enrich egocentric action descriptions, and demonstrate how the enriched descriptions can help the diffusion model understand the action state change from the egocentric perspective.
- We propose a novel model – LEGO that leverages the text and visual embeddings from a visual large language model to improve the performance of the latent diffusion model for egocentric action frame generation.
- We conduct thorough experiments on Ego4D and Epic-Kitchens datasets to validate the superiority of our model over prior approaches. We also showcase the contribution of each component of our model design through ablation studies. We further provide analysis on how the visual instruction tuned embeddings benefit model performance.

2. Related Work

Text-Guided Image Manipulation. The recent emergence of diffusion models enables text-guided image manipulation including image restoration [35], style transfer [76], personalized image synthesis [70, 72, 88], pose generation [30, 38] and generic image editing [16, 19, 36, 40, 45, 59, 62, 80, 83, 83–85, 95, 100, 102]. SDEdit [58] converts the image to the latent space by adding noise through a stochastic differential equation and then denoises the representation for image editing. Rombach *et al.* [69] further expand SDEdit from the original stroke-based editing to text-based editing. Null-text inversion (NTI) [60] inverts a real image by DDIM [37] to yield the diffusion process and then reconstructs the image. The image can then be edited following the same strategies as Prompt-to-Prompt [26]. NTI relies on accurate inversion process which can be improved by using coupled transformations [81] or proximal guidance [25] and accelerated by a blended guidance strategy [63]. To associate the nouns with correct objects, DIFFEDIT [11] generates a mask to localize the manipulated regions. However, most inversion-based methods require accurate image captions, which are largely unavailable in the existing egocentric dataset. Recently, InstructPix2Pix [5] demonstrates the potential to edit a real image without the inversion process and original captions. However, how to leverage the diffusion model to control the state change of an action within the egocentric image plane remains unexplored.

Large Language Model for Image Generation. LLMs [6, 10, 66, 77, 79, 99] and VLLMs [1, 12, 24, 47, 53, 74, 96, 103] have shown their strong capability of understanding complex human instructions. Recently, LLMs and VLLMs are used to guide image generation [2, 7–9, 52, 94, 103]. Wen *et al.* [89] use a pretrained VLLM to pinpoint the misalignment of the text prompt and the synthetic image and then correct it using the diffusion model. Lian *et al.* [50] propose to generate a layout map using an LLM to improve the understanding of prompts with spatial and numeracy reasoning. InstructEdit [84] uses BLIP-2 [47] to infer the

objects that will be edited and then generates a mask with SAM [41] for object grounding. A pre-trained LLM can also be used as a controller to connect with various foundation models [71, 90, 91]. GILL [42] learns text-relevant image embeddings from VLLM in a few additional tokens for image generation. Importantly, all previous efforts leverage the off-the-shelf image or text embeddings from the foundational models. In contrast, our method uses visual instruction tuning to improve the image and text embeddings from the VLLM and thereby facilitates the action frame generation from the egocentric point of view.

Egocentric Vision. Recent efforts seek to understand human’s actions and attentions [17, 31, 32, 39, 43, 44, 49, 75, 87], modeling hand-object interactions [21, 54, 55, 67, 92], and estimating human body poses [48, 57, 78, 82] from the egocentric perspective. Here, we mainly discuss the most relevant works on egocentric visual-language models and egocentric visual content generation. Lin *et al.* [51] propose the first egocentric video-language pre-training model – EgoVLP. Pramanick *et al.* [64] further improve it by incorporating multi-modal fusion directly into the video and language backbone. Ashutosh *et al.* [3] propose to learn a hierarchical video-language embedding for long egocentric videos. Ramakrishnan *et al.* [68] introduce NaQ, which is a data augmentation strategy to train models for long egocentric video search with natural language queries. In terms of egocentric visual generation, Jia *et al.* [34] leverage GANs [20] to generate future head motion in hand forecasting task. Zhang *et al.* [97] leverage GANs to facilitate future gaze anticipation. Ye *et al.* [93] propose the affordance diffusion model that takes in the image of an object and generates possible hand-object interactions in the egocentric view. In this paper, we present the first work that investigates how to leverage VLLMs and diffusion models to generate action state change on the egocentric image plane.

3. Method

The problem setting of egocentric action frame generation is illustrated in Fig. 1(c). Given an egocentric image frame \mathcal{X} that captures the user’s current visual context as well as a user query prompt \mathcal{P} regarding how to perform an action, our goal is to synthesize the action frame \mathcal{Y} that visually depicts how the action should be conducted.

The key insight of our proposed method is leveraging the strong capability of a VLLM to enhance the diffusion model for egocentric action frame generation. The annotations of existing egocentric datasets do not describe the details of how actions are conducted. As a remedy, we leverage visual instruction tuning to finetune a VLLM that enriches action descriptions based on the egocentric visual prompt. In addition, the off-the-shelf CLIP text encoder of a diffusion-based image manipulation model may have a domain gap between the CLIP pre-training data and egocentric action

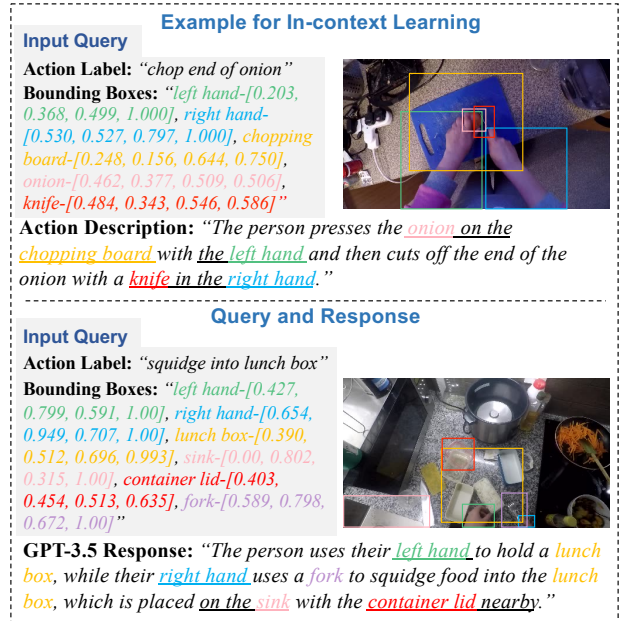


Figure 2. Examples for data curation using GPT-3.5. We provide detailed action descriptions of several example images as well as their action labels and bounding boxes for in-context learning. In addition, we input the action label and bounding boxes of another action as a query. GPT-3.5 is able to generate descriptions with enriched information (highlighted by underlines) in the response.

datasets, resulting in limited understanding of the action-related prompts used in our problem setting. To bridge this gap, we propose LEGO – a novel approach that leverages VLLM embeddings to control the state change of actions and to generate action frames accordingly. We detail the VLLM-based data enrichment pipeline and our model design in the following sections.

3.1. Egocentric Visual Instruction Tuning

Training Data for Visual Instruction Tuning. As shown in Fig. 2, we use GPT-3.5 to generate detailed action descriptions based on an input query composed of a short action label and object bounding boxes. First, we provide several examples of possible inputs along with their expected output descriptions for GPT-3.5 to perform *in-context learning*. These examples cover a diverse set of scenes in the egocentric action dataset. Each example is composed of an action label, a manually annotated action description, and relative spatial information of hands and objects-of-interests represented by bounding box coordinates. GPT-3.5 can learn from the given examples and generate detailed action descriptions based on a new input query. The resulting GPT-3.5 curated data is then further used for visual instruction tuning. More details of the prompt structure are provided in the supplementary.

Visual Instruction Tuning. We follow the finetuning strategy in prior work [53], as shown in Fig. 3(a). Specifically,

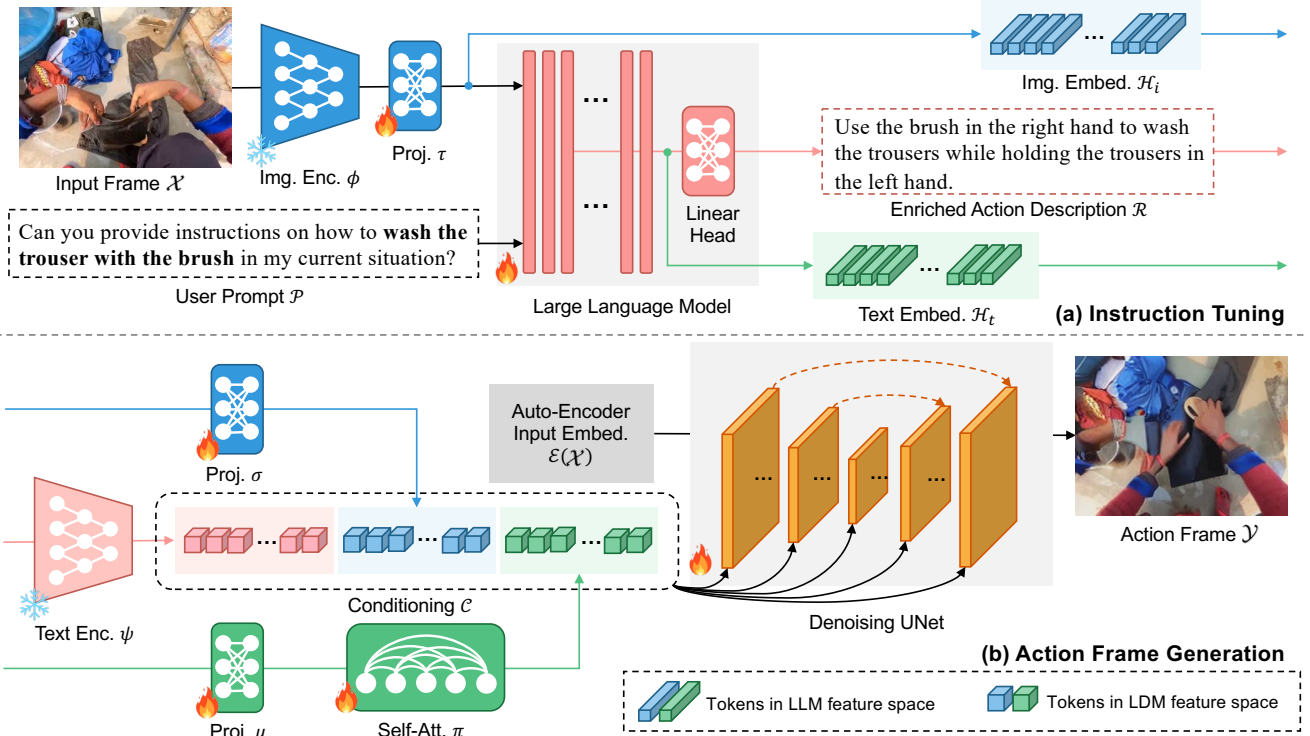


Figure 3. Overview of our proposed LEGO model. We first finetune a visual large language model (VLLM) to generate the enriched action description with visual instruction tuning. We then project image and text embeddings from the finetuned VLLM to the feature space of the latent diffusion model (LDM). Finally, we train the LDM to synthesize the egocentric action frame conditioning on the input frame, enriched action description, as well as the VLLM image and text embeddings.

we use the pre-trained CLIP visual encoder [65] ϕ to encode the visual representation and then apply a linear projection layer τ to map the CLIP visual features into the semantic space of the LLM, *i.e.* $\mathcal{H}_i = \tau(\phi(\mathcal{X}))$. To construct the user prompt \mathcal{P} , we insert the action label annotation into a prompt template to create a coherent query that is aligned with the instruction-following nature of an LLM. We then tokenize \mathcal{P} , and feed both the prompt text tokens and image tokens \mathcal{H}_i as inputs into the LLM. Finally, the LLM is trained to generate enriched action description (denoted as \mathcal{R}) based on the user prompt and image input.

User Prompt Enrichment at Scale. Note that the visual-instruction tuned VLLM doesn't rely on any object bounding boxes as input. Therefore, we can generate enriched action descriptions for all egocentric action data at scale.

3.2. Egocentric Action Frame Generation

We leverage a latent diffusion model (LDM) [69] to synthesize the action frame conditioning on the input frame and the detailed action description \mathcal{R} generated by our finetuned VLLM (see Fig. 3(b)). The input image is first encoded into a latent space using a pre-trained auto-encoder \mathcal{E} . The input to the denoising UNet is a concatenation of the latent input representation $\mathcal{E}(\mathcal{X})$ and a Gaussian noise \mathcal{G} .

Our key innovation is to design the U-Net conditioning

component so that the diffusion model can interpret the enriched action description. To start, we follow [5] and adopt the conventional pre-trained CLIP text encoder ψ to extract a text representation of \mathcal{R} , *i.e.* $\psi(\mathcal{R}) \in \mathbb{R}^{N \times D}$ where N is the maximum number of text tokens and D is the number of feature channels. We further leverage the image and text embeddings from the visual instruction tuned VLLM as additional LDM conditioning to alleviate the domain gap issue of the text encoder.

Specifically, we feed the VLLM image embedding \mathcal{H}_i into an extra linear layer σ to map it to LDM feature space, *i.e.* $\sigma(\mathcal{H}_i) \in \mathbb{R}^{M \times D}$, where M is the number of image tokens. Note that \mathcal{H}_i is already projected to the semantic space during visual instruction tuning, and therefore differs from the image embedding $\mathcal{E}(\mathcal{X})$ from the auto-encoder. Moreover, we also extract the text embedding \mathcal{H}_t before the last linear layer of LLM. We adopt a fixed token number N and enforce padding or truncation behavior, as in the CLIP text encoder. The text embedding is then fed to a projection layer μ . In LLM decoder, the response is generated iteratively and each word embedding only conditions on the context ahead of it. To extract the holistic semantic meaning of \mathcal{H}_t in LDM feature space, we further add self-attention layers π after the projection, *i.e.* $\pi(\mu(\mathcal{H}_t)) \in \mathbb{R}^{N \times D}$. Thus,

the U-Net conditioning can be formulated as:

$$\mathcal{C} = \left[\psi(\mathcal{R}), \sigma(\mathcal{H}_i), \pi(\mu(\mathcal{H}_t)) \right] \in \mathbb{R}^{(2N+M) \times D}. \quad (1)$$

The conditioning \mathcal{C} is fed into the denoising UNet at multiple layers via the cross-attention mechanism [69]. We assume the intermediate feature of a specific UNet layer is \mathcal{U} , which is learned from the UNet input (*i.e.* the concatenation of input frame representation $\mathcal{E}(\mathcal{X})$ and Gaussian noise \mathcal{G}). The cross-attention at this UNet layer can be formulated as:

$$CrossAtt(Q, K, V) = softmax \left(\frac{QK^T}{\sqrt{D}} \right) \cdot V, \quad (2)$$

where $Q = W_Q \cdot \mathcal{U}$, $K = W_K \cdot \mathcal{C}$ and $V = W_V \cdot \mathcal{C}$. Note that W_Q , W_K and W_V are learnable matrices. We also adopt the classifier-free guidance following [5] (see supplementary for details). Finally, the UNet output is converted to the image domain by a pre-trained decoder.

3.3. Implementation Details

All parameters of the VLLM are initialized from the pre-trained LLaVA [53] weights. During training, we freeze the CLIP image encoder and finetune the projection layer and LLM with cross-entropy loss for 3 epochs. To improve the diversity of the text prompts, we randomly select the question template from 10 candidates in each iteration. For LDM training, the text encoder, UNet and auto-encoder are initialized with pre-trained weights [69]. The projection layers σ and μ and the self-attention layers π are initialized using the Xavier algorithm [18]. The text encoder is frozen and the remaining weights are finetuned with L2 regression loss between the predicted noise and real noise for 20,000 iterations. All input and target images are resized to a resolution of 256×256 . Please refer to the supplementary for more details of training and inference.

4. Experiments

We first introduce the datasets, data preprocessing, and evaluation metrics used in our experiments. Then we demonstrate the improvement of our model over prior image manipulation approaches in both quantitative evaluation and qualitative visualization. In addition, we ablate our model to show the contribution of each component. Finally, we investigate the importance of VLLM finetuning to the performance of the diffusion model.

4.1. Data and Metrics

Datasets We conduct our experiments on two well-established egocentric action datasets – Ego4D [22] and Epic-Kitchens [13]. Both datasets were densely annotated with action starting time t and ending time \hat{t} . In our problem setting, we select an egocentric image frame δ_i seconds before the action begins as the input \mathcal{X} , and an image δ_o seconds after the action begins as the target frame

\mathcal{Y} . On the Ego4D dataset, based on the annotations of Pre-Condition-15 time (PRE-15) t_{pre} , and Point-of-No-Return time (PNR) t_{pnr} , we set $\delta_i = t - t_{pre}$ and $\delta_o = t_{pnr} - t$. For Epic-Kitchens, PNR and PRE-15 annotations are not available. Instead, we empirically select $\delta_i = 0.25$ seconds and $\delta_o = t + \lambda * (\hat{t} - t)$, where $\lambda = 0.6$, for our experiments.

Data Preparation for Visual Instruction Tuning. For our dataset curation, we randomly select 20,891 actions with bounding box annotations from the Ego4D training set and 17,922 actions with VISOR [14] mask annotations from the Epic-Kitchens training set. We then insert the original action label into a prompt template to construct the full user prompt. In order to diversify the prompt structure, we prepare 10 prompt templates (see supplementary) and randomly select one for each action at training time.

Data Improvement for Action Frame Generation. Due to the possible drastic camera motion, the egocentric image frames at $t - \delta_i$ and $t + \delta_o$ may be blurry. As a mitigation, we first calculate aesthetic scores [29] of the frames at $t - \delta_i$ and $t + \delta_o$ as well as 3 frames before and after them. The corresponding frames with the highest aesthetic score are used as the input and ground truth of our model. In addition, the egocentric body motion may have huge variance depending on the action type, meaning that the input frame and target frame may look almost identical in more stationary actions (*e.g.* camera wearer is reading book), or significantly different in more active actions (*e.g.* outdoor activities with frequent head motion). Such large variances may incur additional barriers for the diffusion model training. Therefore, we calculate the CLIP similarity of the input frame and target frame, and we filter out the instances where the CLIP similarity is lower than 0.81 or higher than 0.97. With these steps, we ultimately curate 85521/9931 data samples for the train/test sets from Ego4D and 61841/8893 data samples for the train/test sets from Epic-Kitchens.

Metrics. We adopt image-to-image similarity, image-to-text similarity, and user study as metrics in our experiments.

- **Image-to-Image Metrics.** We consider three types of metrics to evaluate image-to-image similarity. (1) Distribution Divergence based metric: Fréchet Inception Distance (FID) [27]. (2) Perception based metrics: Peak Signal-to-Noise Ratio (PSNR) and Learned Perceptual Image Patch Similarity (LPIPS) [98] with SqueezeNet [33] as the encoder. (3) Contrastive pre-training based metrics: image-to-image CLIP score [65], EgoVLP score [51] and EgoVLP+ score [51]. EgoVLP is a contrastive video-language pre-training model trained with egocentric videos. Since EgoVLP takes multiple frames as inputs, we consider two types of inputs: duplicating the output frame as a static input (*i.e.* EgoVLP score) and combining the input frame with the output frame (*i.e.* EgoVLP+ score). As a result, EgoVLP+ can effectively measure whether the generated frame can depict

Methods	Ego4D						Epic-Kitchens					
	CLIP	EgoVLP	EgoVLP+	FID ↓	PSNR	LPIPS ↓	CLIP	EgoVLP	EgoVLP+	FID ↓	PSNR	LPIPS ↓
ProxNPI [25]	0.682	0.445	0.727	33.011	11.876	0.409	0.658	0.323	0.528	51.350	11.064	0.464
SDEdit [58]	0.734	0.501	0.729	33.347	11.813	0.416	0.748	0.338	0.568	27.413	11.296	0.433
IP2P [5]	0.788	0.622	0.788	24.731	12.155	0.372	0.770	0.430	0.611	20.647	11.229	0.408
LEGO	0.806	0.657	0.804	23.830	12.294	0.364	0.786	0.459	0.627	21.566	11.334	0.404

Table 1. Comparison with prior image manipulation approaches. ↓ means a lower score in this metric suggests a better performance. The best results are highlighted with **boldface**. The **green** row refers to our LEGO model performance.

the state change of an action. Note that instead of measuring similarity of input and output frames as in prior works [12, 81], in our problem setting, we measure the similarity between the generated action frame and ground truth, which better reflects whether the generation results can illustrate the execution of an action.

- *Image-to-Text Metrics.* We find the widely-used image-to-text CLIP score can not align actions with egocentric images due to the domain gap. Similar misalignment problem is also observed in [15, 61, 73, 86]. In our experiments, we utilize BLIP [46] to generate image captions of the output images and then calculate text-to-text similarity using CLIP text encoder (following [36]). We implement this metric with two BLIP structures: BLIP-B and BLIP-L. Though this solution may still suffer from the same domain gap issue, it is a more appropriate evaluation metric in our problem setting. See more evidence and discussions in the supplementary.
- *User Study.* We also conduct a user study on a subset of test data to further validate the advantage of our model based on human preference. We sample 60 examples from each dataset and present the generated frames from our model as well as the baseline models to raters on Amazon Mechanical Turk (AMT). We also provide the input frames and the corresponding action labels during evaluation. For each instance, we ask the raters to select the image that best aligned with the provided action label while preserving the most contextual information from the input frame. To minimize potential bias, we hire 5 AMT raters to annotate each example thus resulting in 300 samples for each dataset. The template of our user study is presented in the supplementary.

4.2. Comparison with Prior Approaches

We compare our proposed model with previous state-of-the-art methods for text-guided image manipulation, including ProxNPI [25], SDEdit [58] and InstructPix2Pix (IP2P) [5]. For a fair comparison, we finetune these baseline methods with the same data used in our experiments. Specifically, we train IP2P in an end-to-end way on the two datasets with existing egocentric action labels as text conditioning. ProxNPI and SDEdit rely on the off-the-shelf latent diffusion model to synthesize edited images and thus can not be

Methods	Ego4D		Epic-Kitchens	
	BLIP-B	BLIP-L	BLIP-B	BLIP-L
ProxNPI [25]	0.177	0.174	0.237	0.234
SDEdit [58]	0.198	0.197	0.215	0.213
IP2P [5]	0.200	0.205	0.254	0.264
LEGO	0.204	0.207	0.270	0.274

Table 2. Image-to-text similarity evaluation of our model and baselines. The best results are highlighted with **boldface**.

trained end to end. Therefore, we first finetune the latent diffusion model with egocentric images and action labels and then use the finetuned latent diffusion model parameters to implement ProxNPI and SDEdit approaches.

4.2.1 Quantitative Comparison

As shown in Tab. 1, both ProxNPI and SDEdit perform poorly on this novel problem, suggesting the challenging nature of generating egocentric action frames. IP2P performs much better in almost all metrics by end-to-end training and serves as the strongest baseline model in our experiments. However, our LEGO model consistently outperforms IP2P by a large margin (1.8%, 3.5%, 1.6%, 0.901, 0.139 and 0.8% respectively) in all six metrics on Ego4D. LEGO also exceeds IP2P notably (1.6%, 2.9%, 1.6%, 0.105 and 0.4% respectively) in five metrics on Epic-Kitchens. Though, LEGO slightly lags behind IP2P in FID score, it still achieves the second best performance.

With regard to image-text similarity, LEGO consistently outperforms prior approaches on both datasets (Tab. 2). LEGO outperforms IP2P by 0.4% and 0.2% on Ego4D and by 1.6% and 1.0% on Epic-Kitchens. The result suggests the synthetic frames from our model can better align with the action descriptions. However, the performance gain is rather limited. We emphasize that this is because the domain gap still exists for the BLIP model.

For our user study, we shuffle the order of the results from our model and the baselines while presenting them to the raters. We define the win rate as the percentage of each model being picked as the best out of the total 300 samples. Results are illustrated in Fig. 4. Our model surpasses the second best baseline by 44.0% and 38.3% respectively

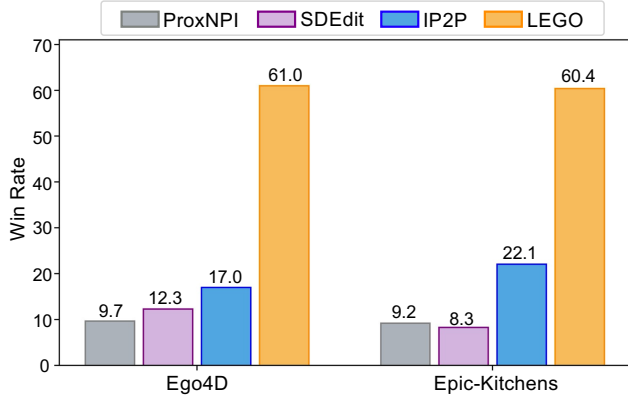


Figure 4. User study of our model and baselines. Win rate is the percentage of each model being picked as the best in all samples. Our model outperforms all baselines by a significant margin.

	Conditioning	CLIP	EgoVLP	EgoVLP+	PSNR
Ego4D	Actions Labels	0.788	0.622	0.788	12.155
	Descriptions	0.791	0.629	0.791	12.200
	Desc. + Img Embed.	0.807	0.654	0.801	12.239
	Desc. + Txt Embed.	0.792	0.633	0.794	12.203
	Desc. + Joint Embed.	0.806	0.657	0.804	12.294
Epic-Kitchens	Actions Labels	0.770	0.430	0.611	11.229
	Descriptions	0.775	0.437	0.615	11.247
	Desc. + Img Embed.	0.785	0.458	0.623	11.254
	Desc. + Txt Embed.	0.777	0.447	0.620	11.305
	Desc. + Joint Embed.	0.786	0.459	0.627	11.334

Table 3. Analysis of egocentric action frame generation performance with different conditionings. Joint Embed. refers to incorporating both VLLM image and text embeddings. The best results are highlighted with **boldface**. The **green** rows refer to our full LEGO model performance.

on Ego4D and Epic-Kitchens. The prominent gap further validates the superiority of our model.

4.3. Visualization of Generated Frames

We additionally showcase examples of generated image from LEGO and baseline models in Fig. 5. ProxNPI and SDEdit fail to understand the user prompt and thus generate frames of irrelevant actions (e.g. row3). They may also easily synthesize the action in a different environment (e.g. row2). InstructPix2Pix is able to preserve more contexts but still fails to semantically align with the action in user prompt (e.g. row4). In contrast, LEGO can synthesize the action frame that better aligns with the user prompt as well as retains more contexts in the background.

4.4. Ablation Study

We present comprehensive ablation studies to investigate the contribution of enriched action descriptions, the VLLM image embedding and the VLLM text embedding sepa-

	Conditioning	CLIP	EgoVLP	EgoVLP+	PSNR
Ego4D	Descriptions	0.791	0.629	0.791	12.200
	Desc.+Img Embed.(w/o FT)	0.804	0.645	0.797	12.238
	Δ (w/o FT - w/ FT)	-0.003	-0.009	-0.004	-0.001
	Desc.+Txt Embed.(w/o FT)	0.791	0.625	0.788	12.154
	Δ (w/o FT - w/ FT)	-0.001	-0.008	-0.006	-0.049
	Desc.+Joint Embed.(w/o FT)	0.802	0.646	0.797	12.222
Δ (w/o FT - w/ FT)	-0.004	-0.011	-0.007	-0.072	
Epic-Kitchens	Descriptions	0.775	0.437	0.615	11.247
	Desc.+Img Embed.(w/o FT)	0.783	0.449	0.620	11.085
	Δ (w/o FT - w/ FT)	-0.002	-0.009	-0.003	-0.169
	Desc.+Txt Embed.(w/o FT)	0.774	0.433	0.610	11.134
	Δ (w/o FT - w/ FT)	-0.003	-0.014	-0.010	-0.171
	Desc.+Joint Embed.(w/o FT)	0.784	0.447	0.619	11.094
Δ (w/o FT - w/ FT)	-0.002	-0.012	-0.008	-0.240	

Table 4. Performance of LEGO without finetuning (w/o FT). The rows highlighted with **gray** indicate the performance drop when compared with results of the counterparts finetuned using visual instruction tuning (w/ FT) from Tab. 3.

ately. Results are demonstrated in Tab. 3. Notably, conditioning on enriched action descriptions can moderately improve the model performance, supporting our claim that expanding the action description can facilitate the learning of the state change during an egocentric action. Moreover, utilizing the image embedding and text embedding from VLLM as additional conditions both improve the model performance by a notable margin. Interestingly, the image embedding leads to larger performance boost on both datasets (e.g. 1.6%/1.0% in CLIP score, and 2.5%/2.1% in EgoVLP score). These results suggest the VLLM image embedding \mathcal{H}_i incorporates important high-level semantic meaning that are not captured in the auto-encoder image embedding $\mathcal{E}(\mathcal{X})$ or VLLM text embedding \mathcal{H}_t . Finally, our full LEGO model uses both VLLM image and text embeddings (Desc.+Joint Embed.) and thus achieves the best performance on both datasets considering all metrics.

4.5. Analysis of Visual Instruction Tuning

We further examine whether the visual instruction tuned embeddings can help the diffusion model to better understand the state change of an egocentric action. As shown in Tab. 4, without any finetuning, the image embedding from the VLLM can still improve the baseline model (*Description*) performance on both datasets. However, the model using off-the-shelf VLLM text embedding actually decreases the baseline model performance. We speculate this is because, the VLLM may generate hallucinated responses without visual instruction tuning, which incurs additional barriers for the text encoder to extract useful information. In addition, finetuned embeddings yield much larger improvement (see the highlighted rows in Tab. 4) across all embeddings types and all metrics (i.e. a relative improvement of 1.7%/2.7% in EgoVLP when using Joint Embed.) on Ego4D/Epic-Kitchens datasets. These



Figure 5. Visualization of the proposed LEGO model and all baselines on Ego4D (the first three rows) and Epic-Kitchens (the last three rows). The action frames generated by LEGO align with the user prompt better and preserve more environment contexts in input frames.

results suggest that visual instruction tuning can align the conditioned embeddings with the instructional prompts and thereby significantly benefit the model performance.

5. Conclusion

In this paper, we introduce the novel problem of egocentric action frame generation. We also propose a novel model — LEGO, that leverages visual instruction tuning and

a diffusion model to address this problem. Our key intuition is to use visual instruction tuning to generate informative responses that depict the execution of the egocentric action, and then design the conditioning of the U-Net to exploit the image and text embeddings from a visual instruction tuned VLLM. Our experiments on two large-scale egocentric action datasets validate the advantage of the proposed approach as well as the contribution of each model component. We believe our

work provides an important step in understanding the action stage change and controllability of diffusion models, and suggests future research directions in egocentric AI systems, image generation, and human skill transfer.

References

- [1] Jean-Baptiste Alayrac, Jeff Donahue, Pauline Luc, Antoine Miech, Iain Barr, Yana Hasson, Karel Lenc, Arthur Mensch, Katherine Millican, Malcolm Reynolds, et al. Flamingo: a visual language model for few-shot learning. *Advances in Neural Information Processing Systems*, 35: 23716–23736, 2022. [2](#)
- [2] Anonymity. Making multimodal generation easier: When diffusion models meet llms. *openreview*, 2023. [2](#)
- [3] Kumar Ashutosh, Rohit Girdhar, Lorenzo Torresani, and Kristen Grauman. Hiervl: Learning hierarchical video-language embeddings. In *Proceedings of the IEEE/CVF Conference on Computer Vision and Pattern Recognition*, pages 23066–23078, 2023. [3](#)
- [4] Joseph H Baskin, Judith G Edersheim, and Bruce H Price. Is a picture worth a thousand words? neuroimaging in the courtroom. *American Journal of Law & Medicine*, 33(2-3): 239–269, 2007. [2](#)
- [5] Tim Brooks, Aleksander Holynski, and Alexei A Efros. Instructpix2pix: Learning to follow image editing instructions. In *Proceedings of the IEEE/CVF Conference on Computer Vision and Pattern Recognition*, pages 18392–18402, 2023. [2](#), [4](#), [5](#), [6](#), [14](#), [16](#)
- [6] Tom Brown, Benjamin Mann, Nick Ryder, Melanie Subbiah, Jared D Kaplan, Prafulla Dhariwal, Arvind Neelakantan, Pranav Shyam, Girish Sastry, Amanda Askell, et al. Language models are few-shot learners. *Advances in neural information processing systems*, 33:1877–1901, 2020. [1](#), [2](#)
- [7] Tuhin Chakrabarty, Kanishk Singh, Arkadiy Saakyan, and Smaranda Muresan. Learning to follow object-centric image editing instructions faithfully. *arXiv preprint arXiv:2310.19145*, 2023. [2](#)
- [8] Junsong Chen, Jincheng Yu, Chongjian Ge, Lewei Yao, Enze Xie, Yue Wu, Zhongdao Wang, James Kwok, Ping Luo, Huchuan Lu, et al. Pixart-alpha: Fast training of diffusion transformer for photorealistic text-to-image synthesis. *arXiv preprint arXiv:2310.00426*, 2023.
- [9] Wei-Ge Chen, Irina Spiridonova, Jianwei Yang, Jianfeng Gao, and Chunyuan Li. Llava-interactive: An all-in-one demo for image chat, segmentation, generation and editing. *arXiv preprint arXiv:2311.00571*, 2023. [2](#)
- [10] Aakanksha Chowdhery, Sharan Narang, Jacob Devlin, Maarten Bosma, Gaurav Mishra, Adam Roberts, Paul Barham, Hyung Won Chung, Charles Sutton, Sebastian Gehrmann, et al. Palm: Scaling language modeling with pathways. *arXiv preprint arXiv:2204.02311*, 2022. [1](#), [2](#)
- [11] Guillaume Couairon, Jakob Verbeek, Holger Schwenk, and Matthieu Cord. Diffedit: Diffusion-based semantic image editing with mask guidance. *arXiv preprint arXiv:2210.11427*, 2022. [2](#)
- [12] Wenliang Dai, Junnan Li, Dongxu Li, Anthony Meng Huat Tiong, Junqi Zhao, Weisheng Wang, Boyang Li, Pascale Fung, and Steven Hoi. Instructblip: Towards general-purpose vision-language models with instruction tuning. *Advances in Neural Information Processing Systems*, 2023. [2](#), [6](#)
- [13] Dima Damen, Hazel Doughty, Giovanni Maria Farinella, Antonino Furnari, Evangelos Kazakos, Jian Ma, Davide Moltisanti, Jonathan Munro, Toby Perrett, Will Price, et al. Rescaling egocentric vision: Collection, pipeline and challenges for epic-kitchens-100. *International Journal of Computer Vision*, pages 1–23, 2022. [2](#), [5](#)
- [14] Ahmad Darkhalil, Dandan Shan, Bin Zhu, Jian Ma, Amran Kar, Richard Higgins, Sanja Fidler, David Fouhey, and Dima Damen. Epic-kitchens visor benchmark: Video segmentations and object relations. In *Proceedings of the Neural Information Processing Systems (NeurIPS) Track on Datasets and Benchmarks*, 2022. [5](#)
- [15] Yilun Du, Sherry Yang, Bo Dai, Hanjun Dai, Ofir Nachum, Joshua B Tenenbaum, Dale Schuurmans, and Pieter Abbeel. Learning universal policies via text-guided video generation. In *Thirty-seventh Conference on Neural Information Processing Systems*, 2023. [6](#)
- [16] Dave Epstein, Allan Jabri, Ben Poole, Alexei A Efros, and Aleksander Holynski. Diffusion self-guidance for controllable image generation. In *Advances in Neural Information Processing Systems*, 2023. [2](#)
- [17] Rohit Girdhar and Kristen Grauman. Anticipative video transformer. In *Proceedings of the IEEE/CVF international conference on computer vision*, pages 13505–13515, 2021. [3](#)
- [18] Xavier Glorot and Yoshua Bengio. Understanding the difficulty of training deep feedforward neural networks. In *Proceedings of the thirteenth international conference on artificial intelligence and statistics*, pages 249–256. JMLR Workshop and Conference Proceedings, 2010. [5](#)
- [19] Vidit Goel, Elia Peruzzo, Yifan Jiang, Dejia Xu, Nicu Sebe, Trevor Darrell, Zhangyang Wang, and Humphrey Shi. Pair-diffusion: Object-level image editing with structure-and-appearance paired diffusion models. *arXiv preprint arXiv:2303.17546*, 2023. [2](#)
- [20] Ian Goodfellow, Jean Pouget-Abadie, Mehdi Mirza, Bing Xu, David Warde-Farley, Sherjil Ozair, Aaron Courville, and Yoshua Bengio. Generative adversarial networks. *Communications of the ACM*, 63(11):139–144, 2020. [3](#)
- [21] Mohit Goyal, Sahil Modi, Rishabh Goyal, and Saurabh Gupta. Human hands as probes for interactive object understanding. In *Proceedings of the IEEE/CVF Conference on Computer Vision and Pattern Recognition*, pages 3293–3303, 2022. [3](#)
- [22] Kristen Grauman, Andrew Westbury, Eugene Byrne, Zachary Chavis, Antonino Furnari, Rohit Girdhar, Jackson Hamburger, Hao Jiang, Miao Liu, Xingyu Liu, et al. Ego4d: Around the world in 3,000 hours of egocentric video. In *Proceedings of the IEEE/CVF Conference on Computer Vision and Pattern Recognition*, pages 18995–19012, 2022. [2](#), [5](#)

- [23] Alon Hafri, John C Trueswell, and Russell A Epstein. Neural representations of observed actions generalize across static and dynamic visual input. *Journal of Neuroscience*, 37(11):3056–3071, 2017. [2](#)
- [24] Jiaming Han, Renrui Zhang, Wenqi Shao, Peng Gao, Peng Xu, Han Xiao, Kaipeng Zhang, Chris Liu, Song Wen, Ziyu Guo, et al. Imagebind-llm: Multi-modality instruction tuning. *arXiv preprint arXiv:2309.03905*, 2023. [2](#)
- [25] Ligong Han, Song Wen, Qi Chen, Zhixing Zhang, Kunpeng Song, Mengwei Ren, Ruijiang Gao, Yuxiao Chen, Di Liu, Qilong Zhangli, et al. Improving negative-prompt inversion via proximal guidance. *Proceedings of the IEEE/CVF Winter Conference on Applications of Computer Vision*, 2024. [2](#), [6](#)
- [26] Amir Hertz, Ron Mokady, Jay Tenenbaum, Kfir Aberman, Yael Pritch, and Daniel Cohen-Or. Prompt-to-prompt image editing with cross attention control. *arXiv preprint arXiv:2208.01626*, 2022. [2](#)
- [27] Martin Heusel, Hubert Ramsauer, Thomas Unterthiner, Bernhard Nessler, and Sepp Hochreiter. Gans trained by a two time-scale update rule converge to a local nash equilibrium. *Advances in neural information processing systems*, 30, 2017. [5](#)
- [28] Jonathan Ho, Ajay Jain, and Pieter Abbeel. Denoising diffusion probabilistic models. *Advances in neural information processing systems*, 33:6840–6851, 2020. [2](#)
- [29] <https://github.com/christophschuhmann/improved-aesthetic-predictor>, 2023. GitHub. [5](#), [16](#)
- [30] Jiancheng Huang, Yifan Liu, Jin Qin, and Shifeng Chen. Kv inversion: Kv embeddings learning for text-conditioned real image action editing. *arXiv preprint arXiv:2309.16608*, 2023. [2](#)
- [31] Yifei Huang, Minjie Cai, Zhenqiang Li, and Yoichi Sato. Predicting gaze in egocentric video by learning task-dependent attention transition. In *Proceedings of the European conference on computer vision (ECCV)*, pages 754–769, 2018. [3](#)
- [32] Yifei Huang, Minjie Cai, Zhenqiang Li, Feng Lu, and Yoichi Sato. Mutual context network for jointly estimating egocentric gaze and action. *IEEE Transactions on Image Processing*, 29:7795–7806, 2020. [3](#)
- [33] Forrest N Iandola, Song Han, Matthew W Moskewicz, Khalid Ashraf, William J Dally, and Kurt Keutzer. Squeezenet: Alexnet-level accuracy with 50x fewer parameters and 0.5 mb model size. *arXiv preprint arXiv:1602.07360*, 2016. [5](#)
- [34] Wenqi Jia, Miao Liu, and James M Rehg. Generative adversarial network for future hand segmentation from egocentric video. In *European Conference on Computer Vision*, pages 639–656. Springer, 2022. [3](#)
- [35] Yitong Jiang, Zhaoyang Zhang, Tianfan Xue, and Jinwei Gu. Autodir: Automatic all-in-one image restoration with latent diffusion. *arXiv preprint arXiv:2310.10123*, 2023. [2](#)
- [36] KJ Joseph, Prateksha Udhayan, Tripti Shukla, Aishwarya Agarwal, Srikrishna Karanam, Koustava Goswami, and Balaji Vasan Srinivasan. Iterative multi-granular image editing using diffusion models. *Proceedings of the IEEE/CVF Winter Conference on Applications of Computer Vision*, 2024. [2](#), [6](#), [14](#)
- [37] Bahjat Kawar, Michael Elad, Stefano Ermon, and Jiaming Song. Denoising diffusion restoration models. In *Advances in Neural Information Processing Systems*, 2022. [2](#)
- [38] Bahjat Kawar, Shiran Zada, Oran Lang, Omer Tov, Huiwen Chang, Tali Dekel, Inbar Mosseri, and Michal Irani. Imagic: Text-based real image editing with diffusion models. In *Proceedings of the IEEE/CVF Conference on Computer Vision and Pattern Recognition*, pages 6007–6017, 2023. [2](#)
- [39] Evangelos Kazakos, Arsha Nagrani, Andrew Zisserman, and Dima Damen. Epic-fusion: Audio-visual temporal binding for egocentric action recognition. In *Proceedings of the IEEE/CVF International Conference on Computer Vision*, pages 5492–5501, 2019. [3](#)
- [40] Sunwoo Kim, Wooseok Jang, Hyunsu Kim, Junho Kim, Yunje Choi, Seungryong Kim, and Gayeong Lee. User-friendly image editing with minimal text input: Leveraging captioning and injection techniques. *arXiv preprint arXiv:2306.02717*, 2023. [2](#)
- [41] Alexander Kirillov, Eric Mintun, Nikhila Ravi, Hanzi Mao, Chloe Rolland, Laura Gustafson, Tete Xiao, Spencer Whitehead, Alexander C Berg, Wan-Yen Lo, et al. Segment anything. *arXiv preprint arXiv:2304.02643*, 2023. [3](#)
- [42] Jing Yu Koh, Daniel Fried, and Ruslan Salakhutdinov. Generating images with multimodal language models. *Advances in Neural Information Processing Systems*, 2023. [3](#)
- [43] Bolin Lai, Miao Liu, Fiona Ryan, and James M Rehg. In the eye of transformer: Global-local correlation for egocentric gaze estimation. *British Machine Vision Conference*, 2022. [3](#)
- [44] Bolin Lai, Fiona Ryan, Wenqi Jia, Miao Liu, and James M Rehg. Listen to look into the future: Audio-visual egocentric gaze anticipation. *arXiv preprint arXiv:2305.03907*, 2023. [3](#)
- [45] Dongxu Li, Junnan Li, and Steven CH Hoi. Blip-diffusion: Pre-trained subject representation for controllable text-to-image generation and editing. *Advances in Neural Information Processing Systems*, 2023. [2](#)
- [46] Junnan Li, Dongxu Li, Caiming Xiong, and Steven Hoi. Blip: Bootstrapping language-image pre-training for unified vision-language understanding and generation. In *International Conference on Machine Learning*, pages 12888–12900. PMLR, 2022. [6](#)
- [47] Junnan Li, Dongxu Li, Silvio Savarese, and Steven Hoi. Blip-2: Bootstrapping language-image pre-training with frozen image encoders and large language models. *International Conference on Machine Learning*, 2023. [2](#)
- [48] Jiaman Li, Karen Liu, and Jiajun Wu. Ego-body pose estimation via ego-head pose estimation. In *Proceedings of the IEEE/CVF Conference on Computer Vision and Pattern Recognition*, pages 17142–17151, 2023. [3](#)
- [49] Yin Li, Miao Liu, and James M Rehg. In the eye of beholder: Joint learning of gaze and actions in first person video. In *Proceedings of the European conference on computer vision (ECCV)*, pages 619–635, 2018. [3](#)

- [50] Long Lian, Boyi Li, Adam Yala, and Trevor Darrell. Llm-grounded diffusion: Enhancing prompt understanding of text-to-image diffusion models with large language models. *arXiv preprint arXiv:2305.13655*, 2023. 2
- [51] Kevin Qinghong Lin, Jinpeng Wang, Mattia Soldan, Michael Wray, Rui Yan, Eric Z XU, Difei Gao, Rong-Cheng Tu, Wenzhe Zhao, Weijie Kong, et al. Egocentric video-language pretraining. *Advances in Neural Information Processing Systems*, 35:7575–7586, 2022. 3, 5
- [52] Bolong Liu, Hao Zhang, Jie Liu, and Qiang Wang. Acigs: An automated large-scale crops image generation system based on large visual language multi-modal models. In *2023 20th Annual IEEE International Conference on Sensing, Communication, and Networking (SECON)*, pages 7–13. IEEE, 2023. 2
- [53] Haotian Liu, Chunyuan Li, Qingyang Wu, and Yong Jae Lee. Visual instruction tuning. *Advances in neural information processing systems*, 2023. 2, 3, 5
- [54] Miao Liu, Siyu Tang, Yin Li, and James M Rehg. Forecasting human-object interaction: joint prediction of motor attention and actions in first person video. In *Computer Vision—ECCV 2020: 16th European Conference, Glasgow, UK, August 23–28, 2020, Proceedings, Part I 16*, pages 704–721. Springer, 2020. 3
- [55] Shaowei Liu, Subarna Tripathi, Somdeb Majumdar, and Xiaolong Wang. Joint hand motion and interaction hotspots prediction from egocentric videos. In *Proceedings of the IEEE/CVF Conference on Computer Vision and Pattern Recognition*, pages 3282–3292, 2022. 3
- [56] Ilya Loshchilov and Frank Hutter. Sgdr: Stochastic gradient descent with warm restarts. In *International Conference on Learning Representations*, 2017. 16
- [57] Zhengyi Luo, Ryo Hachiuma, Ye Yuan, and Kris Kitani. Dynamics-regulated kinematic policy for egocentric pose estimation. *Advances in Neural Information Processing Systems*, 34:25019–25032, 2021. 3
- [58] Chenlin Meng, Yutong He, Yang Song, Jiaming Song, Jiajun Wu, Jun-Yan Zhu, and Stefano Ermon. SDEdit: Guided image synthesis and editing with stochastic differential equations. In *International Conference on Learning Representations*, 2022. 2, 6
- [59] Ashkan Mirzaei, Tristan Aumentado-Armstrong, Marcus A Brubaker, Jonathan Kelly, Alex Levinshtein, Konstantinos G Derpanis, and Igor Gilitschenski. Watch your steps: Local image and scene editing by text instructions. *arXiv preprint arXiv:2308.08947*, 2023. 2
- [60] Ron Mokady, Amir Hertz, Kfir Aberman, Yael Pritch, and Daniel Cohen-Or. Null-text inversion for editing real images using guided diffusion models. In *Proceedings of the IEEE/CVF Conference on Computer Vision and Pattern Recognition*, pages 6038–6047, 2023. 2
- [61] Eyal Molad, Eliahu Horwitz, Dani Valevski, Alex Rav Acha, Yossi Matias, Yael Pritch, Yaniv Leviathan, and Yedid Hoshen. Dreamix: Video diffusion models are general video editors. *arXiv preprint arXiv:2302.01329*, 2023. 6
- [62] Hadas Orgad, Bahjat Kawar, and Yonatan Belinkov. Editing implicit assumptions in text-to-image diffusion models. *arXiv preprint arXiv:2303.08084*, 2023. 2
- [63] Zhihong Pan, Riccardo Gherardi, Xiufeng Xie, and Stephen Huang. Effective real image editing with accelerated iterative diffusion inversion. In *Proceedings of the IEEE/CVF International Conference on Computer Vision*, pages 15912–15921, 2023. 2
- [64] Shraman Pramanick, Yale Song, Sayan Nag, Kevin Qinghong Lin, Hardik Shah, Mike Zheng Shou, Rama Chellappa, and Pengchuan Zhang. Egovlpv2: Egocentric video-language pre-training with fusion in the backbone. In *Proceedings of the IEEE/CVF International Conference on Computer Vision*, pages 5285–5297, 2023. 3
- [65] Alec Radford, Jong Wook Kim, Chris Hallacy, Aditya Ramesh, Gabriel Goh, Sandhini Agarwal, Girish Sastry, Amanda Askell, Pamela Mishkin, Jack Clark, et al. Learning transferable visual models from natural language supervision. In *International conference on machine learning*, pages 8748–8763. PMLR, 2021. 4, 5
- [66] Colin Raffel, Noam Shazeer, Adam Roberts, Katherine Lee, Sharan Narang, Michael Matena, Yanqi Zhou, Wei Li, and Peter J Liu. Exploring the limits of transfer learning with a unified text-to-text transformer. *The Journal of Machine Learning Research*, 21(1):5485–5551, 2020. 1, 2
- [67] Francesco Ragusa, Giovanni Maria Farinella, and Antonino Furnari. Stillfast: An end-to-end approach for short-term object interaction anticipation. In *Proceedings of the IEEE/CVF Conference on Computer Vision and Pattern Recognition*, pages 3635–3644, 2023. 3
- [68] Santhosh Kumar Ramakrishnan, Ziad Al-Halah, and Kristen Grauman. Naq: Leveraging narrations as queries to supervise episodic memory. In *Proceedings of the IEEE/CVF Conference on Computer Vision and Pattern Recognition*, pages 6694–6703, 2023. 3
- [69] Robin Rombach, Andreas Blattmann, Dominik Lorenz, Patrick Esser, and Björn Ommer. High-resolution image synthesis with latent diffusion models. In *Proceedings of the IEEE/CVF conference on computer vision and pattern recognition*, pages 10684–10695, 2022. 2, 4, 5
- [70] Nataniel Ruiz, Yuanzhen Li, Varun Jampani, Yael Pritch, Michael Rubinstein, and Kfir Aberman. Dreambooth: Fine tuning text-to-image diffusion models for subject-driven generation. In *Proceedings of the IEEE/CVF Conference on Computer Vision and Pattern Recognition*, pages 22500–22510, 2023. 2
- [71] Yongliang Shen, Kaitao Song, Xu Tan, Dongsheng Li, Weiming Lu, and Yueting Zhuang. Hugginggpt: Solving ai tasks with chatgpt and its friends in huggingface. *arXiv preprint arXiv:2303.17580*, 2023. 3
- [72] Jing Shi, Wei Xiong, Zhe Lin, and Hyun Joon Jung. Instant-booth: Personalized text-to-image generation without test-time finetuning. *arXiv preprint arXiv:2304.03411*, 2023. 2
- [73] George Stein, Jesse C Cresswell, Rasa Hosseinzadeh, Yi Sui, Brendan Leigh Ross, Valentin Vilecoz, Zhaoyan

- Liu, Anthony L Caterini, J Eric T Taylor, and Gabriel Loaiza-Ganem. Exposing flaws of generative model evaluation metrics and their unfair treatment of diffusion models. *arXiv preprint arXiv:2306.04675*, 2023. 6
- [74] Yixuan Su, Tian Lan, Huayang Li, Jialu Xu, Yan Wang, and Deng Cai. Pandagpt: One model to instruction-follow them all. *arXiv preprint arXiv:2305.16355*, 2023. 2
- [75] Swathikiran Sudhakaran, Sergio Escalera, and Oswald Lanz. Lsta: Long short-term attention for egocentric action recognition. In *Proceedings of the IEEE/CVF Conference on Computer Vision and Pattern Recognition*, pages 9954–9963, 2019. 3
- [76] Zhengwentai Sun, Yanghong Zhou, Honghong He, and PY Mok. Sgdiff: A style guided diffusion model for fashion synthesis. In *Proceedings of the 31st ACM International Conference on Multimedia*, pages 8433–8442, 2023. 2
- [77] Romal Thoppilan, Daniel De Freitas, Jamie Hall, Noam Shazeer, Apoorv Kulshreshtha, Heng-Tze Cheng, Alicia Jin, Taylor Bos, Leslie Baker, Yu Du, et al. Lamda: Language models for dialog applications. *arXiv preprint arXiv:2201.08239*, 2022. 2
- [78] Denis Tome, Thimeo Alldieck, Patrick Peluse, Gerard Pons-Moll, Lourdes Agapito, Hernan Badino, and Fernando De la Torre. Selfpose: 3d egocentric pose estimation from a headset mounted camera. *IEEE Transactions on Pattern Analysis and Machine Intelligence*, 2020. 3
- [79] Hugo Touvron, Thibaut Lavril, Gautier Izacard, Xavier Martinet, Marie-Anne Lachaux, Timothée Lacroix, Baptiste Rozière, Naman Goyal, Eric Hambro, Faisal Azhar, et al. Llama: Open and efficient foundation language models. *arXiv preprint arXiv:2302.13971*, 2023. 2
- [80] Linoy Tsaban and Apolinário Passos. Ledits: Real image editing with ddpm inversion and semantic guidance. *arXiv preprint arXiv:2307.00522*, 2023. 2
- [81] Bram Wallace, Akash Gokul, and Nikhil Naik. Edict: Exact diffusion inversion via coupled transformations. In *Proceedings of the IEEE/CVF Conference on Computer Vision and Pattern Recognition*, pages 22532–22541, 2023. 2, 6
- [82] Jian Wang, Diogo Luvizon, Weipeng Xu, Lingjie Liu, Kripasindhu Sarkar, and Christian Theobalt. Scene-aware egocentric 3d human pose estimation. In *Proceedings of the IEEE/CVF Conference on Computer Vision and Pattern Recognition*, pages 13031–13040, 2023. 3
- [83] Kai Wang, Fei Yang, Shiqi Yang, Muhammad Atif Butt, and Joost van de Weijer. Dynamic prompt learning: Addressing cross-attention leakage for text-based image editing. *arXiv preprint arXiv:2309.15664*, 2023. 2
- [84] Qian Wang, Biao Zhang, Michael Birsak, and Peter Wonka. Instructedit: Improving automatic masks for diffusion-based image editing with user instructions. *arXiv preprint arXiv:2305.18047*, 2023. 2
- [85] Qian Wang, Biao Zhang, Michael Birsak, and Peter Wonka. Mdp: A generalized framework for text-guided image editing by manipulating the diffusion path. *arXiv preprint arXiv:2303.16765*, 2023. 2
- [86] Wen Wang, Kangyang Xie, Zide Liu, Hao Chen, Yue Cao, Xinlong Wang, and Chunhua Shen. Zero-shot video editing using off-the-shelf image diffusion models. *arXiv preprint arXiv:2303.17599*, 2023. 6
- [87] Xiaohan Wang, Linchao Zhu, Heng Wang, and Yi Yang. Interactive prototype learning for egocentric action recognition. In *Proceedings of the IEEE/CVF International Conference on Computer Vision*, pages 8168–8177, 2021. 3
- [88] Yuxiang Wei, Yabo Zhang, Zhilong Ji, Jinfeng Bai, Lei Zhang, and Wangmeng Zuo. Elite: Encoding visual concepts into textual embeddings for customized text-to-image generation. *arXiv preprint arXiv:2302.13848*, 2023. 2
- [89] Song Wen, Guian Fang, Renrui Zhang, Peng Gao, Hao Dong, and Dimitris Metaxas. Improving compositional text-to-image generation with large vision-language models. *arXiv preprint arXiv:2310.06311*, 2023. 2
- [90] Chenfei Wu, Shengming Yin, Weizhen Qi, Xiaodong Wang, Zecheng Tang, and Nan Duan. Visual chatgpt: Talking, drawing and editing with visual foundation models. *arXiv preprint arXiv:2303.04671*, 2023. 3
- [91] Shengqiong Wu, Hao Fei, Leigang Qu, Wei Ji, and Tat-Seng Chua. Next-gpt: Any-to-any multimodal llm. *arXiv preprint arXiv:2309.05519*, 2023. 3
- [92] Yue Xu, Yong-Lu Li, Zheming Huang, Michael Xu Liu, Cewu Lu, Yu-Wing Tai, and Chi-Keung Tang. Egopca: A new framework for egocentric hand-object interaction understanding. In *Proceedings of the IEEE/CVF International Conference on Computer Vision*, pages 5273–5284, 2023. 3
- [93] Yufei Ye, Xueting Li, Abhinav Gupta, Shalini De Mello, Stan Birchfield, Jiaming Song, Shubham Tulsiani, and Sifei Liu. Affordance diffusion: Synthesizing hand-object interactions. In *Proceedings of the IEEE/CVF Conference on Computer Vision and Pattern Recognition*, pages 22479–22489, 2023. 3
- [94] Qifan Yu, Juncheng Li, Wentao Ye, Siliang Tang, and Yueting Zhuang. Interactive data synthesis for systematic vision adaptation via llms-aigcs collaboration. *arXiv preprint arXiv:2305.12799*, 2023. 2
- [95] Zihao Yu, Haoyang Li, Fangcheng Fu, Xupeng Miao, and Bin Cui. Fisedit: Accelerating text-to-image editing via cache-enabled sparse diffusion inference. *arXiv preprint arXiv:2305.17423*, 2023. 2
- [96] Hang Zhang, Xin Li, and Lidong Bing. Video-llama: An instruction-tuned audio-visual language model for video understanding. *arXiv preprint arXiv:2306.02858*, 2023. 2
- [97] Mengmi Zhang, Keng Teck Ma, Joo Hwee Lim, Qi Zhao, and Jiashi Feng. Deep future gaze: Gaze anticipation on egocentric videos using adversarial networks. In *Proceedings of the IEEE conference on computer vision and pattern recognition*, pages 4372–4381, 2017. 3
- [98] Richard Zhang, Phillip Isola, Alexei A Efros, Eli Shechtman, and Oliver Wang. The unreasonable effectiveness of deep features as a perceptual metric. In *Proceedings of the IEEE conference on computer vision and pattern recognition*, pages 586–595, 2018. 5
- [99] Susan Zhang, Stephen Roller, Naman Goyal, Mikel Artetxe, Moya Chen, Shuohui Chen, Christopher Dewan, Mona Diab, Xian Li, Xi Victoria Lin, et al. Opt: Open pre-trained transformer language models. *arXiv preprint arXiv:2205.01068*, 2022. 1, 2

- [100] Shu Zhang, Xinyi Yang, Yihao Feng, Can Qin, Chia-Chih Chen, Ning Yu, Zeyuan Chen, Huan Wang, Silvio Savarese, Stefano Ermon, et al. Hive: Harnessing human feedback for instructional visual editing. *arXiv preprint arXiv:2303.09618*, 2023. [2](#)
- [101] Yuxin Zhang, Nisha Huang, Fan Tang, Haibin Huang, Chongyang Ma, Weiming Dong, and Changsheng Xu. Inversion-based style transfer with diffusion models. In *Proceedings of the IEEE/CVF Conference on Computer Vision and Pattern Recognition*, pages 10146–10156, 2023. [2](#)
- [102] Zhixing Zhang, Ligong Han, Arnab Ghosh, Dimitris N Metaxas, and Jian Ren. Sine: Single image editing with text-to-image diffusion models. In *Proceedings of the IEEE/CVF Conference on Computer Vision and Pattern Recognition*, pages 6027–6037, 2023. [2](#)
- [103] Deyao Zhu, Jun Chen, Xiaoqian Shen, Xiang Li, and Mohamed Elhoseiny. Minigt-4: Enhancing vision-language understanding with advanced large language models. *arXiv preprint arXiv:2304.10592*, 2023. [2](#)

LEGO: Learning EGOcentric Action Frame Generation via Visual Instruction Tuning

Supplementary Material

This is the supplementary material for the paper titled "LEGO: Learning EGOcentric Action Frame Generation via Visual Instruction Tuning". We organize the content as follows:

A – Analysis of Image-to-Text Metrics

B – Quality of the Enriched Action Descriptions

C – Additional Experiment Results

C.1 – Performance at Different Transition Time

C.2 – Effect of Dataset Scale

C.3 – Generation of New Actions

C.4 – Additional Visualization

D – More Implementation Details

D.1 – Prompt and Examples for Data Curation

D.2 – Examples of Data Preprocessing

D.3 – Visual Instruction Tuning

D.4 – Egocentric Action Frame Generation

D.5 – User Study of Generated Action Frames

E – Limitation and Future Work

F – Code and Data Release

A. Analysis of Image-to-Text Metrics

In Tab. 5, we report the image-to-text CLIP score of InstructPix2Pix (IP2P) [5] baseline and the ground truth. Ideally, the CLIP score between the ground truth and the text prompt should serve as a performance upperbound (UB). However, the upperbound image-to-text CLIP score is very close to the baseline on Ego4D, and even lower than the baseline on Epic-Kitchens. It suggests the CLIP model fails to align action descriptions with corresponding egocentric images in semantics, thus resulting in a quick saturation in CLIP score. In our experiments, we use BLIP to caption the generated image and measure the text-to-text similarity of captions and action descriptions (following [36]). The two metrics (BLIP-B and BLIP-L) that use two different BLIP structures both result in larger gap between the baseline model and the upperbound (3.7%/3.0% vs. 0.9% and 1.6%/1.4% vs. -1.1%). Therefore, we adopt BLIP based metrics and user study to measure image-text alignment. Note that, our model still performs on-par or slightly better than IP2P in image-to-text CLIP score, and exceeds IP2P notably when using BLIP based metrics and user study (see Tab. 2 and Fig. 4 in the main paper).

B. Quality of the Enriched Action Descriptions

In our approach, we finetune a visual large language model (VLLM) using visual instruction tuning to generate en-

Methods	Ego4D			Epic-Kitchens		
	CLIP	BLIP-B	BLIP-L	CLIP	BLIP-B	BLIP-L
IP2P [5]	0.205	0.200	0.205	0.217	0.254	0.264
UpperBound (UB)	0.214	0.237	0.235	0.206	0.270	0.278
$\Delta = \text{UB} - \text{IP2P}$	0.009	0.037	0.030	-0.011	0.016	0.014

Table 5. Image-to-text metrics of the baseline model and upperbound. The gray row shows the gap of IP2P to the upperbound. The upperbound measured by CLIP score is comparable with or even lower than the baseline model (highlighted by red).

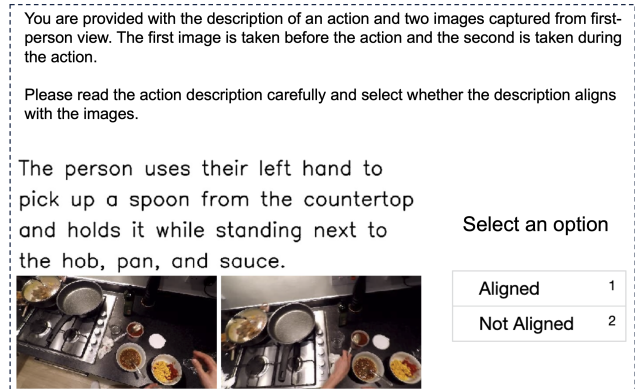


Figure 6. The interface used for evaluation of enriched action descriptions. Both input and target frames are shown to the raters.

riched action descriptions. Here, we provide additional analysis on the quality of generated action descriptions using user study. We randomly sample 100 examples from the test set of each dataset. For each instance, we show the input frame, target frame and the action descriptions from VLLM. The rater is asked to select whether the description aligns with the two frames. We hire 5 raters for each instance on Amazon Mechanical Turk and finally get 500 samples for each dataset. The interface shown to raters is illustrated in Fig. 6. The percentage of samples with aligned frames and action descriptions is 87.0% on Ego4D and 84.0% on Epic-Kitchens. The results suggest the visual instruction tuned VLLM can effectively expand action labels with details captured in the input frame.

C. Additional Experiment Results

C.1. Performance at Different Transition Time

As explained in Sec. 4.1 of main paper, for an action beginning at t , we select the frame at $t - \delta_i$ as input and the frame at $t + \delta_o$ as target. We divide the test data into

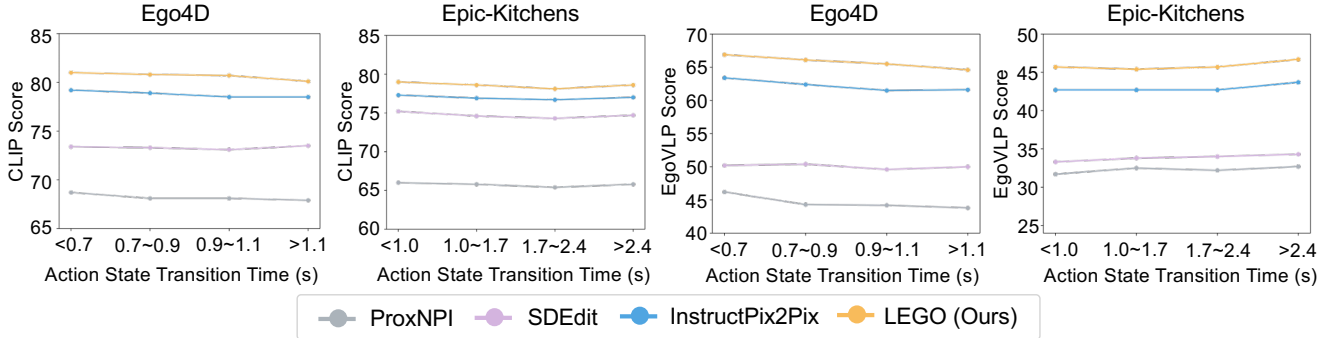


Figure 7. Comparison with baselines at different action transition time. Our model outperforms all baselines across all transition time.

Methods	Ego4D						Epic-Kitchens					
	CLIP	EgoVLP	EgoVLP+	FID ↓	PSNR	LPIPS ↓	CLIP	EgoVLP	EgoVLP+	FID ↓	PSNR	LPIPS ↓
LEGO	0.806	0.657	0.804	23.830	12.294	0.364	0.786	0.459	0.627	21.566	11.334	0.404
LEGO (scaleup)	0.809	0.663	0.808	23.560	12.301	0.363	0.789	0.475	0.635	19.635	11.400	0.399

Table 6. Comparison of LEGO trained with single dataset and both datasets (denoted as *scaleup*). ↓ means a lower score in this metric suggests a better performance. The better results are highlighted with **boldface**. The performance of LEGO model can be effectively improved by involving more training data.

four bins according to the action state transition time from input frame to target frame $\delta = \delta_i + \delta_o$. We establish the threshold for each bin to ensure that the quantity of data samples in each bin is relatively similar. The performance of LEGO and baselines at different transition time is demonstrated in Fig. 7. The flat curves suggest the egocentric action frame generation problem is equally challenging regardless of transition time. Our model still surpasses all baselines by a notable margin across all transition time. This fine-grained result further validates the superiority of our approach.

C.2. Effect of Dataset Scale

We further analyze how the dataset scale affects our model performance by merging the training set of Ego4D and Epic-Kitchens. The training strategy and other hyperparameters remain identical to separate training on each dataset. We demonstrate the results in Tab. 6. The performance of our model is further boosted by leveraging more training data (*i.e.* *scaleup*). Notably, the gains on Epic-Kitchens are more prominent than gains on Ego4D (*e.g.* 1.6% vs. 0.6% on EgoVLP score, 1.931 vs. 0.270 on FID, *etc.*). The possible reason is that Ego4D dataset has more training data covering more diverse scenarios and actions. Hence, it can greatly compensate for the low diversity of Epic-Kitchens dataset after merging them. The improvement on two datasets suggests our model can be effectively boosted by scaling up the training data.

C.3. Generation of New Actions

In addition to generating action frames based on the pre-defined action descriptions in our datasets, we validate whether our approach is able to synthesize the action frames conditioning on the same contexts yet different actions (novel image-action pairs). Results are illustrated in Fig. 8. We feed different actions with the same input frame to our model. The synthesized frames correctly depict the execution of the actions in the same environment. This result further indicates that our model can understand the action state change and generalize to different user queries.

C.4. Additional Visualization

We demonstrate more results from our model and the ground truth in Fig. 11. The generated frames are well aligned with the user query and the ground truth except some typical failure cases (last two rows). Our approach may fail to associate the action with the correct objects when the objects are not distinct enough in the egocentric perspective, *e.g.* the *marker* and *croissant* in the first row of failure cases. In addition, generating the action frame in some scenarios needs more contexts than a static input frame. For example, the model fails to understand which object is the furniture and incorrectly drives the nails into the wood under it (*i.e.* the second failure case of Ego4D). It also lacks the context that the user already holds a bag of noodles, so it synthesizes a frame of taking out the noodles from a cupboard (*i.e.* the second failure case of Epic-Kitchens). These weaknesses can inspire more future studies in egocentric action frame generation. Please refer to



Figure 8. Visualization of generating various actions from the same input frame. The first action (“open drawer”) is the existing label for this example in the dataset. We fill another five actions into the user query and synthesize the action frames using our model. All generated frames align well with the actions and preserve most contexts provided by the user.

Appendix E for more discussions.

D. More Implementation Details

D.1. Prompt and Examples for Data Curation

In data curation, we randomly select 12 examples from each datasets covering diverse scenarios. All examples are shown in Fig. 13 and Fig. 14. We also clarify our requirements in the prompt sent to GPT-3.5. The complete prompt is shown in Fig. 9. We specify the composition of input query, the expected detailed information and extra requirements for the output in the system information. Then we input the examples for in-context learning and the example for inference in the user input.

D.2. Examples of Data Preprocessing

For each input frame or target frame, we calculate aesthetic scores [29] of the current frame as well as 3 frames before and after (7 frames in total). As demonstrated in Fig. 12(a), the frame of the highest aesthetic score usually has the best image quality. We then use this frame as input or target frame. We also calculate the similarity of input and target frame for each action. We empirically filter out data whose similarity is lower than 0.81 or higher than 0.97. Some examples of abandoned data are shown in Fig. 12(b). A very low similarity usually indicates a big change in the background due to the head motion. A very high similarity implies the action involves very small hand movements. It’s hard for generative models to learn action generation in these data samples.

D.3. Visual Instruction Tuning

We train the model with a batch size of 128 and a learning rate of 2×10^{-5} . Warm-up strategy and cosine anneal [56] are also used in training. It takes 24 hours to train the model

on 8 NVIDIA A100-SXM4-40GB for 3 epochs. Please refer to Fig. 8 for the example of incorporating action label into action instruction query templates.

D.4. Egocentric Action Frame Generation

We finetune the latent diffusion model with a batch size of 256 and an initial learning rate of 10^{-4} without warm-up strategy. Horizontal flipping is used as data augmentation during training. We train the model for 20,000 iterations on 8 NVIDIA A100-SXM4-40GB over 38 hours. In inference, we apply 100 denoising steps for each instance.

We also use classifier-free guidance for two conditions (following [5]) by sharing the same guidance scale across the enriched action descriptions, VLLM image embeddings and VLLM text embeddings. As defined in Sec. 3.2 in main paper, we use \mathcal{C} to denote the three conditions and use \mathcal{X} to denote the input frame. Specifically, we randomly set only the image conditioning $\mathcal{X} = \emptyset$ at a probability of 5%, only the conditioning from VLLM $\mathcal{C} = \emptyset$ at a probability of 5% and both $\mathcal{X} = \emptyset$ and $\mathcal{C} = \emptyset$ at a probability of 5%. Then the score estimate of our model is

$$\tilde{e}_\theta(z_t, \mathcal{X}, \mathcal{C}) = e_\theta(z_t, \emptyset, \emptyset) \quad (3)$$

$$+ s_x \cdot (e_\theta(z_t, \mathcal{X}, \emptyset) - e_\theta(z_t, \emptyset, \emptyset)) \quad (4)$$

$$+ s_c \cdot (e_\theta(z_t, \mathcal{X}, \mathcal{C}) - e_\theta(z_t, \mathcal{X}, \emptyset)), \quad (5)$$

where θ refers to the parameters in the denoising UNet. z_t is the noisy latent at timestep t , which is obtained by diffusion process in training and randomly initialized by a gaussian noise in inference. s_x and s_c are the guidance scales corresponding to the conditioning \mathcal{X} and \mathcal{C} respectively. In inference, we use $s_x = 7.5$ and $s_c = 1.5$ which are identical to the settings in InstructPix2Pix [5].

System: You are an AI assistant that provides a description of an image based on the action and object context. The action consists of a verb and nouns. Each object location is represented by a bounding box. For each bounding box, four numbers are provided in brackets – they are [x-coordinate of top-left, y-coordinate of top-left, x-coordinate of bottom-right, y-coordinate of bottom-right]. The origin is at the top-left of each frame. The x-axis is on the top and the y-axis is on the left. All coordinates are normalized to the range from 0 to 1. This information can be used to infer the spatial relation of hands and objects. Note that the detailed narration is in a natural and holistic style. Please add more details in the action. For example, try to describe which hand is used in each action like “with right hand” or “using left hand”. Try to describe the spatial relation of these objects like “on the right”, “on the left”, “from ... to ...” or use some spatial words like “in”, “on”, “out”, “front”, “back”, etc. Describe the image in only one sentence. Do not describe objects or actions that are not presented in action or objects locations context. Many examples are provided for learning and an additional example is provided for inference.

User: Examples for learning: (1) {Example-1} (2) {Example-2} ... (12) {Example-12}

User: Example for inference: {Inference Example}

Figure 9. The structure of the prompt sent to GPT-3.5. We specify the composition of the input query (highlighted in blue). Then we articulate the requirements for action enrichment (highlighted in green) and extra demands (highlighted in yellow). Example-1 to Example-12 consist of the action label, object bounding boxes and manual annotation of detailed action descriptions. The inference example consists of just action label and object bounding boxes.

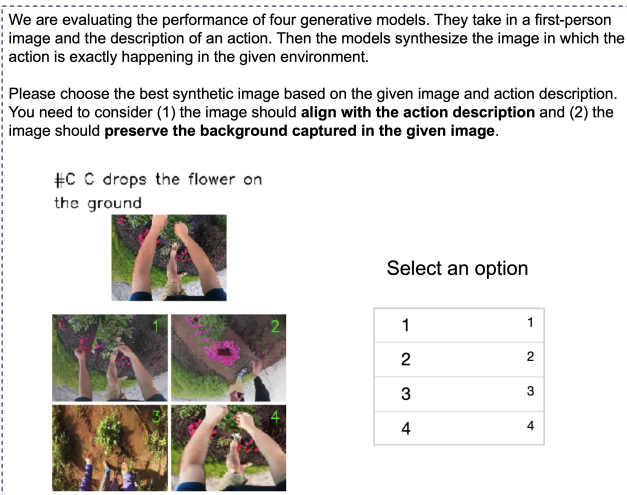


Figure 10. The interface used for evaluation of generated action frames. The four generated frames are randomly shuffled to avoid potential bias.

D.5. User Study of Generated Action Frames

The user interface for evaluation of generated action frames is illustrated in Fig. 10. We show the input frame and shuffled outputs from four models to raters. To make a fair comparison, we show the action label instead of the enriched action description because the baseline models only take original action labels as input.

E. Limitation and Future Work

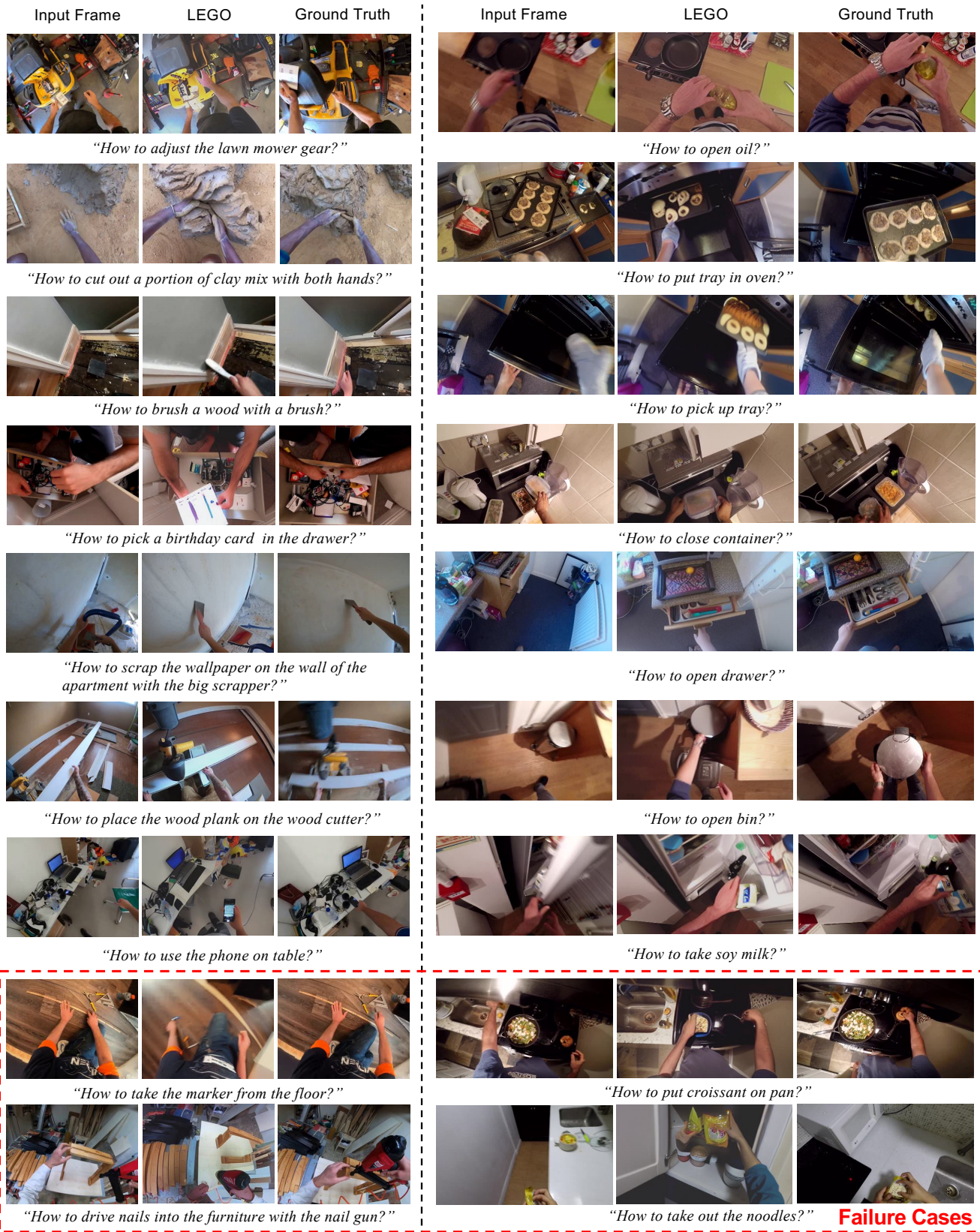
In this paper, we use an egocentric image to capture the user’s environment contexts and generate the action frame to provide visual instructions. However, there are still some problems that are not explicitly solved by our method. We find it’s hard for our model to associate the action with correct objects when there are too many irrelevant objects around. Synthesizing the diverse and complex hand-object interactions is also a big challenge especially when people are operating some machines. In addition, our work indicates a few valuable directions for the future study.

- The embeddings from visual large language model (VLLM) are fed into the UNet together with the CLIP based text representation. How to leverage the VLLM embeddings more effectively in diffusion models deserves future study.
- Recognizing and localizing the objects that are relevant with the action descriptions in a chaotic environment may be a bottleneck for the application in real-world problems, which deserves more attention.
- It’s difficult to synthesize correct interactions of hands and objects in some professional work, such as using a wood cutter, operating a lawn mower and sewing clothes on a sewing machine. How to combine affordance understanding with generative models may be a key step to address this problem.
- Existing automatic image-to-text similarity metric doesn’t generalize well to the egocentric domain. We

expect more investigation of better evaluation metrics for image-text alignment.

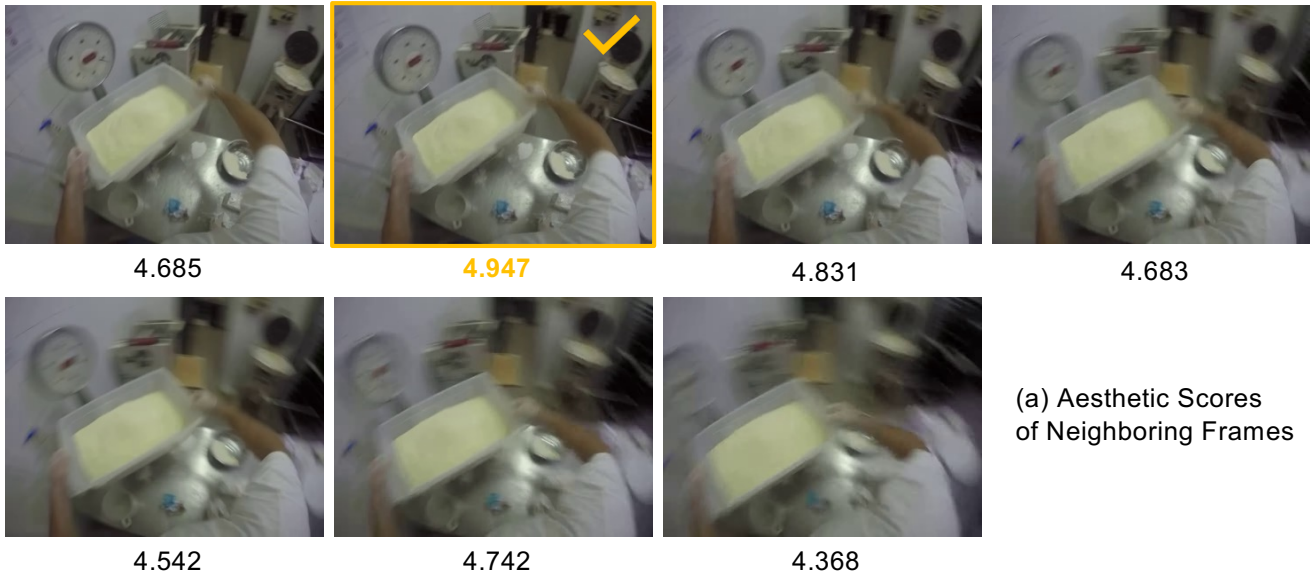
F. Code and Data Release

The code, pre-trained model weights, additional data annotations and our train/test split will be made publicly available to the research community to facilitate future studies.

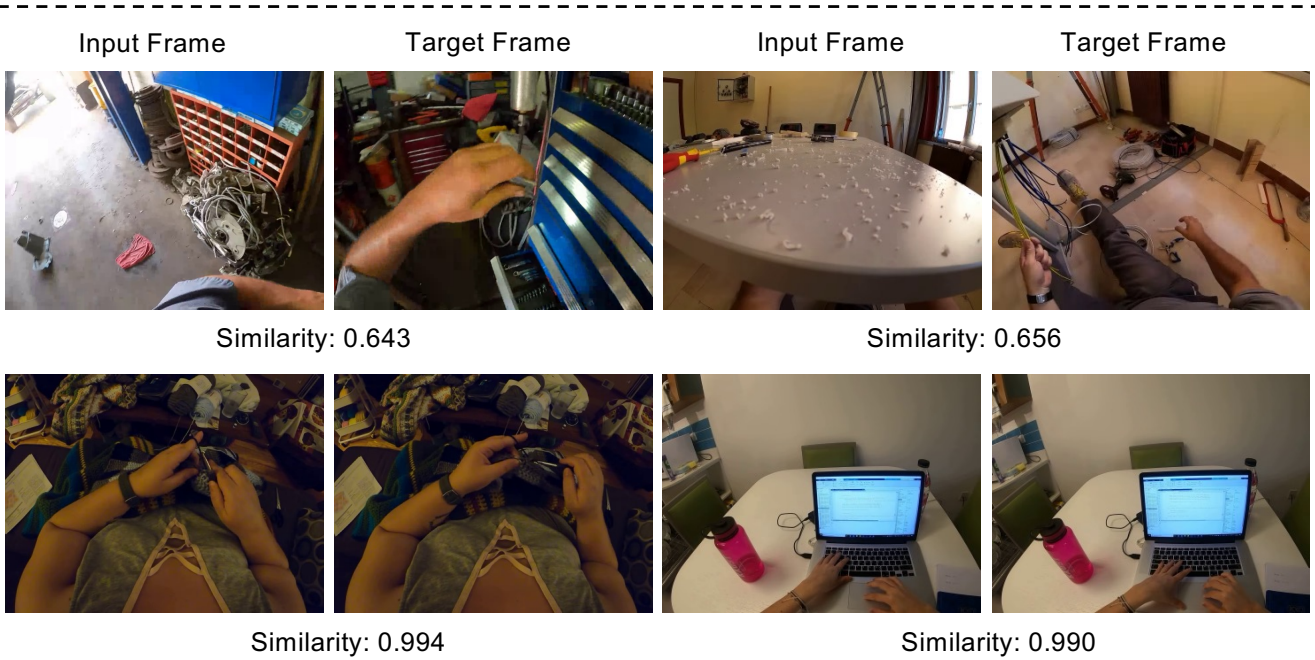


Failure Cases

Figure 11. Additional visualization of LEGO output on Ego4D (on the left of the dash line) and Epic-Kitchens (on the right of the dash line). We also show the ground truth for reference. In the last two rows, we demonstrate some failure cases on the two datasets.

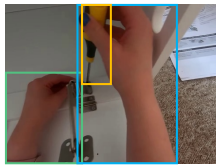


(a) Aesthetic Scores of Neighboring Frames

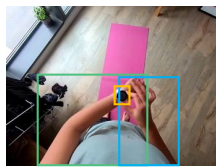


(b) Examples with Very Low and Very High Similarity of Input and Target Frames

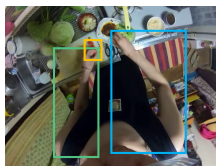
Figure 12. Data preprocessing in our work. (a) The frame with the highest aesthetic score (highlighted) is less blurry and then used as the target frame of this action. (b) The actions with too low (<0.81) or too high similarity (>0.97) between input and target frames are filtered out from the datasets.



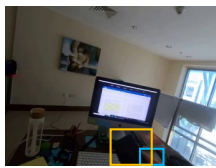
Action Label: "tighten the nut"
Bounding Boxes: (shown on image)
Action Descriptions: "The person holds the nut using the left hand and tightens it with the screwdriver in the right hand."



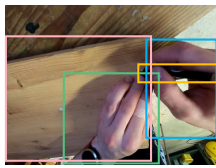
Action Label: "adjust wrist watch"
Bounding Boxes: (shown on image)
Action Descriptions: "The person uses the right hand to adjust the wrist watch wore on the left wrist."



Action Label: "drop the slice of tomato on a plate"
Bounding Boxes: (shown on image)
Action Descriptions: "The person drops the slice of tomato in the right hand on a plate on the right."



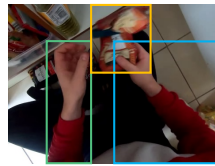
Action Label: "pick phone"
Bounding Boxes: (shown on image)
Action Descriptions: "The person picks the phone using the right hand."



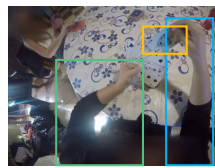
Action Label: "mark the wood"
Bounding Boxes: (shown on image)
Action Descriptions: "The person presses the wood using the left hand and makes a mark using the pencil in the right hand."



Action Label: "check on a fabric"
Bounding Boxes: (shown on image)
Action Descriptions: "The person reaches out to a fabric using the right hand and checks its status by touching it."



Action Label: "shake something"
Bounding Boxes: (shown on image)
Action Descriptions: "The person holds and shakes something in the right hand."



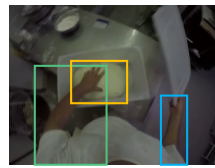
Action Label: "place the card in between other cards"
Bounding Boxes: (shown on image)
Action Descriptions: "The person uses the right hand to place the card in other cards held in the left hand."



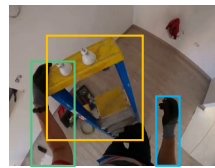
Action Label: "drop the game console on the table"
Bounding Boxes: (shown on image)
Action Descriptions: "The person drops the game console in hands on the table."



Action Label: "attach the second screw to the first bicycle with his right hand"
Bounding Boxes: (shown on image)
Action Descriptions: "The person attaches the screw in the right hand to the bike."



Action Label: "press dough in container with left hand"
Bounding Boxes: (shown on image)
Action Descriptions: "The person uses the left hand to press the dough in a container in front of him."



Action Label: "go up the ladder"
Bounding Boxes: (shown on image)
Action Descriptions: "The person holds on to the ladder using the left hand and goes up the ladder."

Figure 13. All Ego4D examples used for data curation from GPT-3.5 via in-context learning. For simplicity, the bounding boxes are only shown on images. We input the coordinates of bounding boxes to GPT-3.5 in practice.



Figure 14. All Epic-Kitchens examples used for data curation from GPT-3.5 via in-context learning. For simplicity, the bounding boxes are only shown on images. We input the coordinates of bounding boxes to GPT-3.5 in practice.